Interaction of Profilin with G-Actin and Poly(L-proline)

Irina Perelroizen, Jean-Baptiste Marchand, Laurent Blanchoin, Dominique Didry, and Marie-France Carlier*

Laboratoire d'Enzymologie, CNRS, 91198 Gif-sur-Yvette Cedex, France

Received March 14, 1994; Revised Manuscript Received May 12, 1994•

ABSTRACT: The interaction of bovine spleen profilin with ATP- and ADP-G-actin and poly(L-proline) has been studied by spectrofluorimetry, analytical ultracentrifugation, and rapid kinetics in low ionic strength buffer. Profilin binding to G-actin is accompanied by a large quenching of tryptophan fluorescence, allowing the measurement of an equilibrium dissociation constant of 0.1–0.2 μM for the 1:1 profilin–actin complex, in which metal ion and nucleotide are bound. Fluorescence quenching monitored the bimolecular reaction between G-actin and profilin, from which association and dissociation rate constants of 45 μM^{-1} s^{-1} and 10 s^{-1} at 20 °C could be derived. The tryptophan(s) which are quenched in the profilin–actin complex are no longer accessible to solvent, which points to W356 in actin as a likely candidate, consistent with the 3D structure of the crystalline profilin–actin complex [Schutt, C. E., Myslik, J. C., Rozycki, M. D., Goonesekere, N. C. W., & Lindberg, U. (1993) *Nature 365*, 810–816]. Upon binding poly(L-proline), the fluorescence of both tyrosines and tryptophans of profilin is enhanced 2.2-fold. A minimum of 10 prolines [three turns of poly(L-proline) helix II] is necessary to obtain binding (K_D = 50 μM), the optimum size being larger than 10. Binding of poly(L-proline) is extremely fast, with $k_+ > 200$ μM^{-1} s^{-1} at 10 °C. Neither the affinity nor the rate of association of G-actin to profilin, nor the promotion of actin assembly by profilin in the presence of thymosin β_4 [Pantaloni, D., & Carlier, M.-F., (1993) *Cell 75*, 1007–1014], are affected by poly(L-proline). These results are discussed in relation with profilin structure and function *in vivo*.

Profilin is a small (12–15 kDa) actin binding protein (Carlsson *et al.*, 1977) present in all eukaryotic cells in fairly large amounts (5×10^{-6} to 5×10^{-5}M). Genetic studies indicate that *in vivo* profilin plays an essential role in the processes of actin assembly involved in a number of vital motile functions such as early development in *Drosophila* (Cooley *et al.*, 1992), formation of fruiting body in *Dictyostelium discoideum* (Haugwitz *et al.*, 1993), and establishment of the proper cell polarity in yeast *Sacharomyces cerevisiae* (Haarer *et al.*, 1990). In addition to its binding to G-actin, profilin also binds to L-α-phosphatidylinositol 4,5-biphosphate (PIP_2) (Lassing & Lindberg, 1985; Goldschmidt-Clermont *et al.*, 1990) and to poly(L-proline) (Tanaka & Shibata, 1985; Lindberg *et al.*, 1988), which led to the suggestion [see Machesky and Pollard (1993) for review] that it has the potential to mediate a link between the signaling pathways operating at the plasma membrane and the localized actin assembly occurring in response to stimuli. The localization of at least part of the profilin at the leading edge of locomoting fibroblasts (Buss *et al.*, 1992) and at the rear of *Listeria monocytogenes* during its propulsive movement in the host cytoplasm (Thériot *et al.*, 1994) supports this potential function. It is thought that site-directed actin assembly in response to cell stimulation is made possible by the existence of two mains pools of actin in motile cells: the pool of polymerized F-actin and the pool of monomeric sequestered actin, maintained unpolymerized by interaction with G-actin binding proteins such as Tβ_4 (Safer *et al.*, 1991). Part of the population of sequestered G-actin is shifted into the pool of F-actin when the cells are stimulated. Recent *in vitro* experiments (Pantaloni & Carlier, 1993) have shown that profilin promotes F-actin assembly off the pool of G-actin–Tβ_4 complex. This effect is due to the lowering of the steady-state concentration of G-actin by profilin and occurs as a consequence of the reported (Pollard & Cooper, 1984; Pring *et al.*, 1992) participation of profilin–actin complex in filament assembly at the barbed end. When barbed ends are blocked, profilin simply acts as a G-actin sequestering, F-actin depolymerizing agent. These results reconcile the apparent discrepancies concerning the *in vivo* effects of profilin on actin assembly (Cooley *et al.*, 1992; Haugwitz *et al.*, 1993; Haarer *et al.*, 1990; Cao *et al.*, 1992; Finkel *et al.*, 1994). They also led to the proposal (Pantaloni & Carlier, 1993; Carlier & Pantaloni, 1994) that the regulation of site-directed actin assembly is exerted via a control of the G-actin steady-state concentration, in two opposite fashions, by capping proteins and profilin.

The essential roles of profilin outlined above, its interactions with multiple ligands, and potential complex functional regulation argue for the detailed understanding of its structure–function relationship. The recent determination of the 3D structure of profilin by NMR (Vinson *et al.*, 1993) and X-ray crystallography (Schutt *et al.*, 1993; Cedergren-Zeppezauer *et al.*, 1994) has been a breakthrough in this respect. Interestingly, the structure of all profilins appears highly conserved despite sequence variability and clearly shows distinct binding sites for actin, poly(L-proline), and PIP_2. Moreover, the actin binding site which is thought to correspond to the very tight contact between the two proteins in the crystalline profilin–actin complex (Schutt *et al.*, 1993) does not contain the conserved sequences initially thought to be part of the actin binding site. The large variability in the reported affinities (10^7–10^5 M^{-1}) of profilin for G-actin contrasts with the conserved structure of the interface between the two proteins. What part of this variability is due to intrinsic differences between different profilins/actins, or to the methodologies used, remains unclear.

In the present work, we propose novel fluorimetric methods to measure the binding parameters of actin and poly(L-proline) to profilin and characterize the functional properties of the ternary actin–profilin–poly(L-proline) complex. These methods will be useful, once combined with site-directed mutagenesis, to elucidate profilin function at the molecular level.

• Abstract published in *Advance ACS Abstracts,* July 1, 1994.

0006-2960/94/0433-8472$04.50/0

MATERIALS AND METHODS

Proteins. Actin was purified from rabbit muscle (Spudich *et al.*, 1971) and isolated as CaATP-G-actin though Sephadex G-200 chromatography (McLean-Fletcher & Pollard, 1980) in G buffer (5 mM Tris-Cl⁻, pH 7.8, 0.1 mM $CaCl_2$, 0.2 mM DTT, 0.2 mM ATP 0.01% NaN_3). MgATP-G-actin was prepared by preincubation of CaATP-G-actin (~10 μM) with 50 μM $MgCl_2$ and 0.2 mM EGTA for 5 min at 0 °C (Carlier *et al.*, 1986) and diluted at the desired concentration in G buffer also supplemented with EGTA and $MgCl_2$. ADP-G-actin was prepared as described (Carlier *et al.*, 1984), kept on ice, and used within 4 h in G buffer containing either $CaCl_2$ or $MgCl_2$ + 0.2 mM EGTA, 25 μM ADP, and 10 μM Ap_5A to inhibit myokinase activity. Actin was pyrenyl labeled as described (Kouyama & Mihashi, 1981).

Profilin was purified from bovine spleen by poly(L-proline) affinity chromatography (Lindberg *et al.*, 1988; Kaiser *et al.*, 1989). Briefly, ~250 g frozen spleen (cut into 2 × 2 × 5 cm pieces and rapidly frozen on dry ice at the slaughter house and then kept at −80 °C until use) were homogenized with 350 mL of H buffer containing 10 mM Tris-Cl⁻, pH 7.8, 100 mM glycine, 100 mM KCl, 1 mM DTT, 0.5% Triton X100, and 1 mM PMSF. The homogenate was centrifuged for 30 min at 20000*g* and then for 105 min at 125000*g* and directly loaded onto the poly(L-proline) column. Following washings with buffer A (buffer H without triton X100) and buffer A containing 4 M urea, profilin (~25 mg) was eluted with buffer A containing 7 M urea. Profilin was immediately dialyzed extensively against 5 mM Tris-Cl⁻, pH 7.8, containing 1 mM DTT, concentrated to 200–300 μM using a Centriprep 10 ultrafiltration apparatus (Amicon), centrifuged at 400000*g* for 15 min at 4 °C in a TL100 ultracentrifuge (Beckman), stored at 0 °C, and used within 3 weeks without any sign of deterioration.

Thymosin β_4 was purified from ovine spleen as previously described (Carlier *et al.*, 1993).

Fluorescence Measurements. Static fluorescence studies were carried out in a Spex Fluorolog 2 spectrofluorimeter. Titrations of G-actin by profilin were performed either adding consecutive small amounts of profilin to a cuvette containing G-actin at a concentration of 0.2–1.5 μM, keeping the total volume increase lower than 2%, or by preparing different samples containing the same amount of G-actin and different amounts of profilin. The two techniques gave identical results. Small cuvettes were used (4-mm light path) to minimize screen effect, which was undetectable, at 1.5 μM G-actin, up to 10 μM profilin. Excitation and emission wavelengths were 295 and 330 nm, respectively.

Rapid kinetics of interaction of G-actin with profilin were monitored using a stopped-flow apparatus (DX-17 MV, Applied Photophysics) with fluorescence detection. The excitation slit was 0.5 mm (2 nm), the excitation wavelength was 295 nm, and a KV 320 Schott filter was placed on the emission beam. Temperature was 20 or 10 °C as indicated. All concentrations indicated are final concentrations after mixing.

Sedimentation Velocity Studies. Sedimentation velocity of G-actin, profilin, and the profilin-actin complex was performed in a XLA Beckman analytical ultracentrifuge, at 20 °C and 60 000 rpm with absorbance monitoring at 280 nm.

Polymerization Measurements. The amount of F-actin at steady-state was derived from pyrene fluorescence measurements, using a very low proportion of labeled actin (1.5%). Samples containing actin, $T\beta_4$, profilin, and poly(L-proline) at the indicated concentrations in polymerization buffer (i.e., G buffer supplemented with 2 mM $MgCl_2$ and 0.1 M KCl) were assayed following overnight incubation at 20 °C, as described previously (Pantaloni & Carlier, 1993).

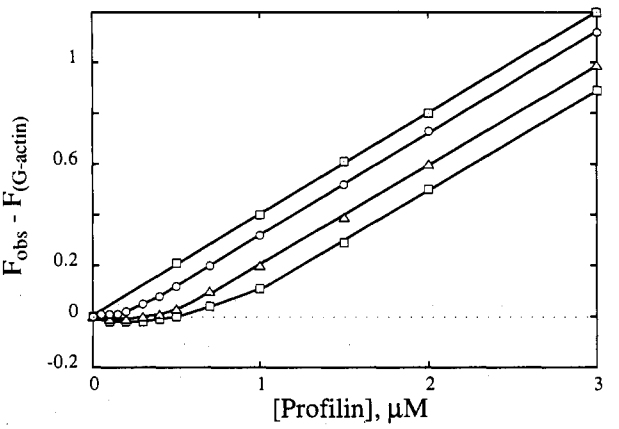

FIGURE 1: Quenching of tryptophan fluorescence associated to the formation of profilin–actin complex. Profilin was added, at the indicated concentrations, to solutions containing CaATP-G-actin at the following concentrations (μM): G, 0; E, 0.16; C, 0.36; G, 0.53. The fluorescence of G-actin was substracted in each series of samples. The solid lines are theoretical curves calculated according to eqs 1 and 3 using K_P = 0.12 μM, F_A = 1, F_P = 0.2, and F_{PA} = 0.91.

RESULTS

A Change in Tryptophan Fluorescence Accompanies the Formation of the Profilin–Actin Complex. When increasing amounts of profilin were added to a solution of G-actin in G buffer containing 10–50 μM ATP, the observed fluorescence intensity of tryptophans was lower than the sum of the intensities measured for each of the two proteins alone. Data are shown in Figure 1. At saturating amounts of profilin, the fluorescence extrapolated to a straight line parallel to the calibration curve obtained with profilin alone. The data could be analyzed within the formation of a 1:1 complex between G-actin and profilin, in which the fluorescence of tryptophans would be quenched, as follows:

$$F_{obs} = F_A[A] + F_P[P] + F_{PA}[PA] \quad (1)$$

where F_{obs} is the observed fluorescence intensity, and F_A, F_P, and F_{PA} are the intrinsic fluorescences of free G-actin, free profilin, and profilin–actin complex, respectively. The mass conservation equations are

$$[A]_{tot} = [A] + [PA]$$

$$[P]_{tot} = [P] + [PA] \quad (2)$$

Equation 1 could be written

$$\Delta F = F_{obs} - F_A[A]_{tot} - F_P[P]_{tot} = (F_{PA} - F_A - F_P)([PA] = \Delta\varphi[PA] \quad (3)$$

ΔF therefore was proportional to the concentration of PA complex, and the dependence of ΔF on $[P]_{tot}$ at different concentrations $[A]_{tot}$ could be analyzed as binding isotherms to derive the equilibrium dissociation K_p for the profilin–actin complex. Using a reference value of 1 for F_A, values of 0.2 and 0.91 were derived for F_P and F_{PA}, respectively, and the best fit of all data shown at 0.16, 0.36, and 0.53 μM G-actin was obtained for a value of K_p of 0.12 μM. These results therefore demonstrate that, in a low ionic strength buffer, the

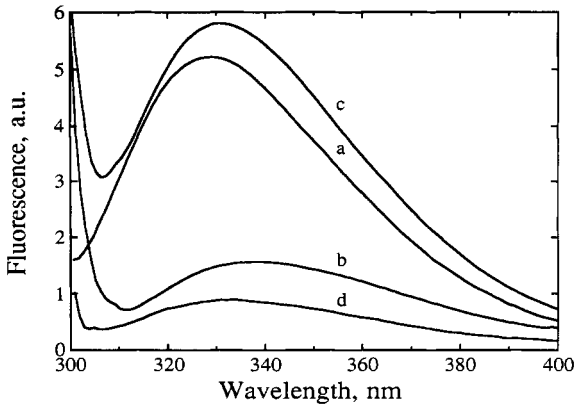

FIGURE 2: Fluorescence emission spectra of tryptophans in G-actin, profilin, and profilin–actin complex. Tryptophan fluorescence was excited at 295 nm. The following emission spectra are shown: a, G-actin alone (1 μM); b, profilin alone (1.4 μM); c, G-actin + profilin mixed at the same concentrations as in a and b; d, difference spectrum (a + b − c) showing that the maximum fluorescence change upon interaction between profilin and actin is observed at 330 nm.

high affinity ($\sim 10^7$ M^{-1}) binding of profilin to G-actin is monitored by a quenching of $100[1 - [0.91/(1 + 0.2)]]\% = 24\%$ of tryptophan fluorescence. In other independent experiments carried out with different preparations of actin and profilin, the value of K_p varied from 0.1 to 0.25 μM.

The same experiment was carried out with MgATP-G-actin and MgADP-G-actin. Identical values of K_p and F_{PA} were obtained in all cases. Typically, superimposable titration curves were obtained, under the exact same conditions when ATP- or ADP-G-actin was used.

From the fluorescence emission spectra of G-actin alone, profilin alone, and both proteins mixed, the difference spectrum corresponding to the profilin–actin complex could be derived and is shown on Figure 2. The maximum emission wavelength for monitoring the profilin–actin complex was 330 nm. The above results do not *a priori* tell us whether the tryptophans whose fluorescence is quenched in the complex belong to profilin or to G-actin, or to both. However, the crystallized structure of the profilin–actin complex (Schutt *et al.*, 1993) shows that neither one of the two conserved tryptophans in profilin (W3 and W31) belong to the primary actin–profilin close contact. In addition, the structure of profilin does not appear modified when it interacts with G-actin (Schutt *et al.*, 1993; Metzler *et al.*, 1993; Cedergren-Zeppezauer *et al.*, 1994); hence it is more likely that the fluorescence quenching observed in the profilin–actin complex reflects a change in the environment of tryptophans belonging to actin.

To clarify this point, the accessibility of tryptophans to solvent in actin, profilin, and profilin–actin complex was assayed by measuring the dynamic quenching of tryptophane fluorescence by KCl. Data displayed in Figure 3 show that the fluorescence of G-actin tryptophans is partly quenched by KCl, while no such quenching was observed in the profilin–actin complex, which indicates that the tryptophan(s) of G-actin which are accessible to solvent and are dynamically quenched by KCl are no longer exposed to solvent in the profilin–actin complex. The extent of fluorescence quenching of profilin tryptophans by KCl was much smaller than what was measured for G-actin (compare closed triangles and open circles in Figure 3). The fractional maximum solvent-accessible fluorescence of G-actin, i.e., the fluorescence of the tryptophan(s) buried in the profilin–actin complex, can be derived from the ordinate intercept in the modified Stern–Volmer plot (Lehrer, 1971) of the collisional quenching of G-actin by KCl (Figure 3, inset). A value of $^1/_4$ was found.

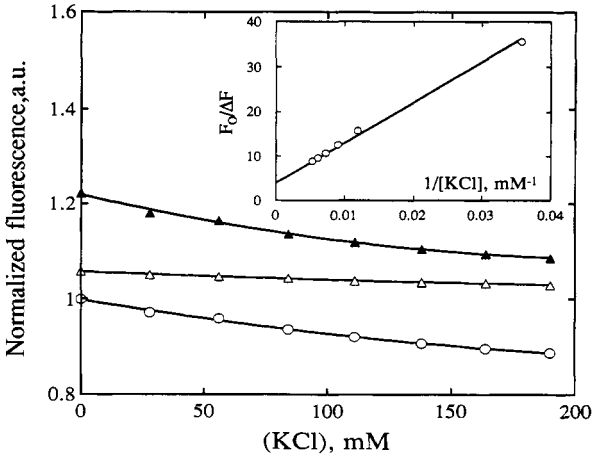

FIGURE 3: Solvent accessibility of tryptophans of free G-actin and profilin–actin complex. Tryptophan fluorescence was measured after addition of KCl at the indicated concentrations to G-actin (2 μM) in the absence (○) or the presence (△) of 2.2 μM profilin. Closed triangles (▲) represent the sum of the measured fluorescences of profilin alone and G-actin alone at different KCl concentrations. (Inset) Modified Stern–Volmer plot (Lehrer, 1971) of the collisional quenching of G-actin fluorescence by KCl.

Therefore, the actin tryptophan(s) quenched in the profilin–actin complex contribute 25% of the overall G-actin fluorescence. In agreement with the above data, when the interaction between G-actin and profilin was assayed by fluorescence in polymerization buffer containing 0.1 M KCl, the fluorescence quenching was too small to yield a reliable titration curve.

Kinetic Analysis of Profilin–Actin Interaction. The change in tryptophan fluorescence linked to profilin–actin interaction was used as a probe to monitor the time course of complex formation in the stopped-flow apparatus. Kinetic analysis of the signal is expected to give information on the mechanism leading to the fluorescence change. Typical fluorescence traces are displayed in Figure 4A. The time course of fluorescence change was recorded at a constant CaATP-G-actin concentration (1 μM) and a series of profilin concentrations up to 10 μM. When profilin was in excess over G-actin, the fluorescence decrease was an exponential process and the observed first-order rate constant increased linearly with the concentration of profilin, indicating that the change in tryptophan fluorescence simply monitors the bimolecular reversible reaction of profilin with G-actin, as described below:

$$P + A \underset{k_{-p}}{\overset{k_{+p}}{\rightleftharpoons}} PA$$

The pseudo-first-order observed rate constant is $k_{obs} = k_{+p}[P]_{tot} + k_{-p}$. From the slope of the linear increase of k_{obs} versus $[P]_{tot}$ (Figure 4B), values of 45 ± 5 and 25 ± 3 μM^{-1} s^{-1} were derived for k_{+p} at 20 °C and 10 °C, respectively. The value of k_{-p} could be derived from the ordinate intercept with a relatively large uncertainty ($\sim$5–20 s^{-1}). However, combining the kinetic data with the value of the equilibrium dissociation constant $K_P = k_{-p}/k_{+p} = 0.2 \pm 0.05$ μM derived from analysis of the amplitude of the fluorescence change (Figure 4C) led to a more accurate value of k_{-p} of 10 ± 5 s^{-1}.

Kinetics of binding of profilin to MgATP-G-actin led to values of k_{+p} and k_{-p} identical to the ones above. The interaction of MgADP-G-actin with profilin led to the exact same extent of quenching of tryptophane fluorescence and the same value of the equilibrium dissociation constant as with ATP-G-actin. On the other hand, the association and

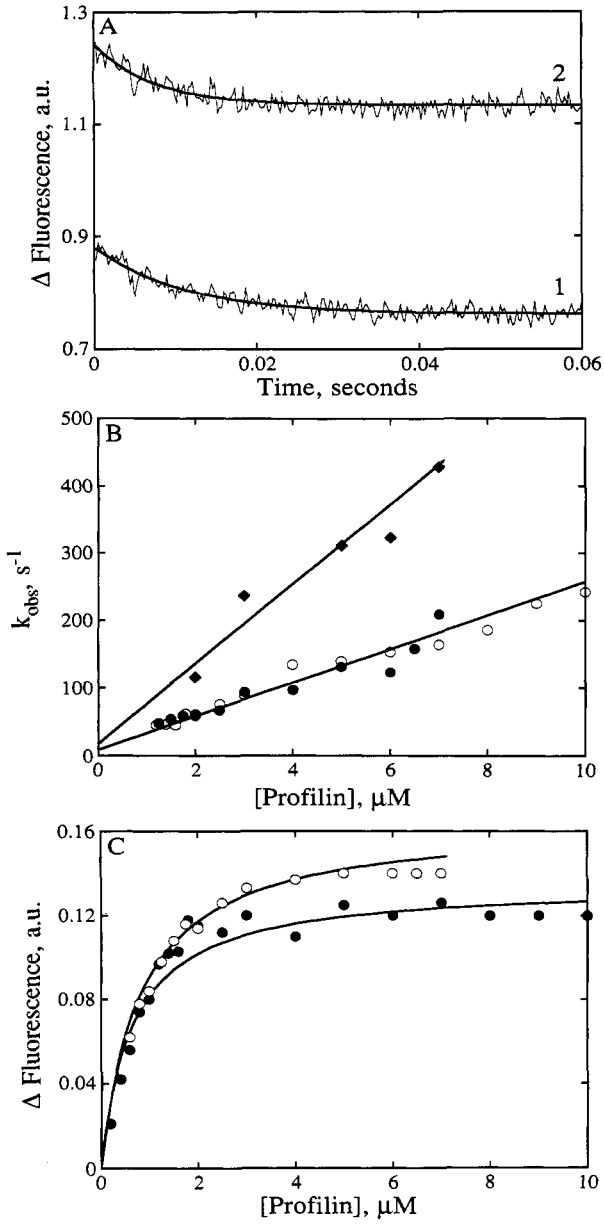

FIGURE 4: Rapid kinetics of complex formation between G-actin and profilin. The kinetics of fluorescence decrease upon binding of profilin at different concentrations to G-actin (1 μM) was monitored at 10 °C in the stopped-flow apparatus. (Panel A) Typical recorded time courses of binding of G-actin (1 μM) to profilin (3 μM, lower trace; 4 μM, upper trace). The continuous line represents the best fit to an exponential process. (Panel B) Plot of the pseudo-first-order rate constant of the fluorescence change versus profilin concentration. Circles: reaction of ATP-G-actin (1 μM) with profilin containing (○) or not (●) 0.2 mg/mL poly(L-proline). Squares: Reaction of ADP-G-actin (1 μM) with profilin. (Panel C) Amplitude of the fluorescence change versus total concentration of profilin (●) in the absence of poly(L-proline) and (○) in the presence of 0.4 mg/mL poly(L-proline) in the syringe containing profilin.

dissociation rate constants were twice larger for interaction of profilin with ADP-G-actin than with ATP-G-actin (Figure 4B).

Kinetic data therefore indicate that the change in tryptophan fluorescence accompanying the formation of the profilin–actin complex occurs very rapidly upon the formation of the contact between the two proteins, and is not linked to a slower subsequent conformation change. This result too suggests that the quenched tryptophan(s) is (are) in the close vicinity of the interface between the two proteins.

Analysis of Profilin–Actin Interaction by Sedimentation Velocity. The structure of crystalline profilin–actin (Schutt *et al.*, 1993) indicates that profilin may bind a second actin molecule. In this second weaker contact (1110 Å^2 buried interfacial area) the N-terminal helix of profilin interacts with subdomain 4 of actin. A search for a possible ternary complex of G-actin with two profilins was carried out using sedimentation velocity. Samples containing 8 μM G-actin and increasing concentrations of profilin up to 100 μM were run in the analytical ultracentrifuge. A single 1:1 profilin–actin complex was clearly observed with a sedimentation coefficient of 3.95–4 S at 20 °C in all samples. The sedimentation coefficients of G-actin and profilin were 3.4 and 1.9 S, respectively, under the same conditions. At the highest profilin concentration, the formation of even less than 4 μM actin–(profilin)$_2$ would not have escaped attention; hence we can conclude that the affinity of profilin for actin at the putative second binding site is certainly weaker than 10^4 M^{-1} under our experimental conditions.

Nucleotide and Divalent Cation Bound to G-Actin in the Profilin–Actin Complex. It has been well established (Mockrin & Korn, 1980; Nishida, 1985; Goldschmidt-Clermont *et al.*, 1991, 1992) that profilin increases the rates of Ca^{2+} and ATP dissociation from G-actin. It is therefore possible that the affinity of Ca-ATP for actin is reduced upon profilin binding, if the corresponding association rate constants are not increased to the same extent. A lower affinity of CaATP for actin in the profilin–actin complex must be linked to a corresponding increased affinity of profilin for actin without CaATP bound, as specified by thermodynamic detailed balance.

The observation (Lindberg *et al.*, 1988) that the tight profilactin complex, which represents a minor (~15%) fraction of profilin in different cellular extracts, has no nucleotide bound, is supportive of this view. It is important to check that the concentrations of CaATP in the 10^{-6}–10^{-5}M range used in this work are sufficient to ensure saturation of the nucleotide site in the PA–CaATP complex studied above. Two control experiments were performed. G-actin (10 μM) was dialyzed against G buffer containing 5 μM $CaCl_2$ and 5 μM ATP, in which either calcium ions or ATP were traced with $^{45}CaCl_2$ or [^{3}H]ATP. G-actin was then chromatographed over Sephadex G-25 (PD-10, Pharmacia) equilibrated with dialysis buffer, as described (Valentin-Ranc & Carlier, 1989), in the presence or absence of 20 μM profilin. It was checked that the same amount of either ^{45}Ca or [^{3}H]ATP was bound to the actin or actin + profilin peak eluting from the columns (data not shown), which guaranteed that the profilin–actin complex studied in the present work is the profilin–actin–metal–nucleotide complex. Within these results, the affinity of CaATP for actin in the profilin–actin complex is at least 10^6 M^{-1}.

Binding of Poly(L-proline) to Profilin and Characterization of a Ternary Complex Poly(L-proline)–Profilin–Actin. Poly(L-proline) is known to be a ligand of profilin (Tanaka & Shibata, 1985), a property used in the profilin purification procedure (Lindberg *et al.*, 1988). The structure of the crystalline profilin–actin complex (Schutt *et al.*, 1993) as well as mutagenesis studies (Haarer *et al.*, 1993; Björkegren *et al.*, 1993) attribute the poly(L-proline) binding site of profilin to a group of solvent-exposed hydrophobic conserved residues comprising W3, Y6, W31, H133, L134, and Y139. The presence of the two tryptophans and of two of the four tyrosines of profilin suggests that changes in intrinsic fluorescence of profilin should suitably monitor its interaction with poly(L-

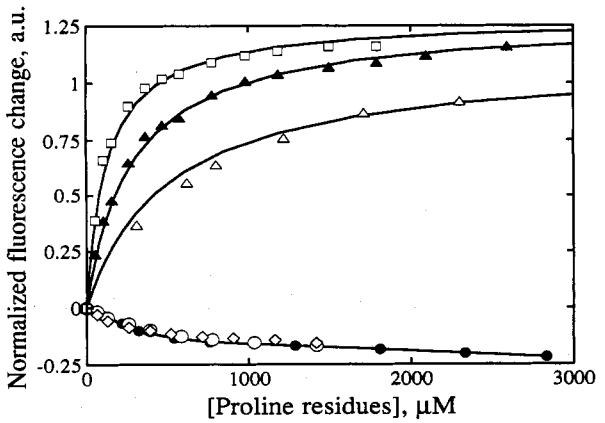

FIGURE 5: Change in profilin fluorescence upon binding poly(L-proline). Titration curves of profilin (1 μM) by poly(L-proline) containing different average numbers n of proline residues per polypeptide chain were carried out as described under Materials and Methods. (◊) $(pro)_4$; (●) $(Pro)_6$; (○) $(Pro)_8$; (△) $(Pro)_{10}$; (□) poly-L-Pro 1000–10 000 (MW = 5600; n = 50); (▲) poly-L-pro 15 000–30 000 (MW = 15 000, n = 130).

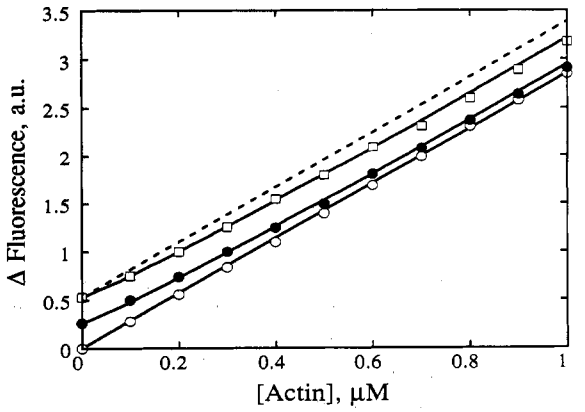

FIGURE 6: Evidence for a ternary complex G-actin–profilin–poly-(L-proline). The fluorescence of G-actin (λ_{exc} 295 nm, λ_{em} 330 nm) was measured at the indicated concentrations in the absence (○) and in the presence (●) of 0.5 μM profilin. 350 μM poly(L-proline) (Pro_{10}) was then added to each sample, and the fluorescence was again measured (□). The dashed line indicates the theoretical linear change in fluorescence expected after addition of an excess of poly(L-proline), within mutual exclusion binding of G-actin and poly(L-proline) to profilin.

proline). Excitation fluorescence spectra (not shown) demonstrated that the fluorescences of both tyrosines (λ^{exc}_{max} = 275 nm) and tryptophans (λ^{exc}_{max} = 295 nm) were enhanced 2.2-fold upon poly(L-proline) binding. The extent of tyrosine fluorescence change was the greater. Poly(L-proline)s of different degrees of polymerization were assayed, in order to determine the minimum number of prolines required for efficient binding to profilin. Data displayed in Figure 5 show that the increase in tyrosine fluorescence (λ_{exc} 275 nm; λ_{em} 320 nm) is a saturation function of poly(L-proline). $(Pro)_4$, $(Pro)_6$, and $(Pro)_8$ were unable to cause an increase in profilin fluorescence and instead caused a small quenching, maybe due to collisional effects. $(Pro)_{10}$ did bind to profilin, in agreement with a previous report (Machesky & Pollard, 1993), and induced a slightly lower (2-fold) fluorescence enhancement than the one observed with poly(L-proline)s of higher degree of condensation. The equilibrium dissociation constants (in terms of molarity of proline residues) were 500 μM for $(Pro)_{10}$ (corresponding to an intrinsic K_D of 50 μM) and 125 and 275 μM for the poly(L-proline)s containing on average 50 and 130 proline residues, respectively. The change of K(proline) with the average number of covalently linked proline residues (not shown) indicates that the optimum size for efficient binding is an oligomer of 15–20 proline residues, which would bind with an estimated intrinsic K_D of $\sim$5 μM. The rate constant for poly(L-proline) binding to profilin was too high to be determined using the stopped-flow apparatus. The fluorescence change was complete within the dead-time (0.8 ms) of the instrument even at low concentrations (20 μM) of poly-(L-proline), leading to a minimum estimated value of 200 μM^{-1} s^{-1} for poly(L-proline) binding to profilin.

It has been proposed, on the basis of poly(L-proline) binding (Machesky & Pollard, 1993; Schutt *et al.*, 1993), that profilin could play a role similar to that of proteins involved in signaling pathways which contain SH_3 domains able to interact with proline-rich sequences of target proteins in the transduction cascade. In particular, a 4-fold-repeated sequence containing four prolines exists in the *Listeria* surface protein ActA which is necessary for actin assembly and bacterium propulsion (Kocks *et al.*, 1992); this sequence was thought to be involved in the recruitment of profilin at the surface of *Listeria* (Thériot *et al.*, 1994). A 20 amino acid peptide of Act A (297–316) containing the proline-rich sequence was synthesized. This peptide failed to cause an increase in fluorescence of profilin and did not inhibit the binding of poly(L-proline) when added at concentrations up to 1 mM (7 mM proline residues).

Assuming that binding to a poly(L-proline) sequence in an unknown protein is responsible for anchoring profilin to some regions of the cell cortex, thus localizing the promotion of actin assembly at the barbed ends, it is essential to determine how binding of poly(L-proline) quantitatively affects profilin interaction with G-actin and its function as a motor of actin assembly. The following experiments were carried out to address these issues.

First, evidence was obtained, using the fluorescence assay, for a ternary complex between profilin, G-actin, and poly-(L-proline), as opposed to a mutual exclusion scheme. Samples containing different concentrations of G-actin in the range 0–1 μM were prepared. Fluorescence was assayed before and after the addition of profilin (0.5 μM) and then following a subsequent addition of a large amount (0.4 mg/mL) of poly(L-proline) (n = 10). Data are displayed in Figure 6. The final fluorescence was obviously different from the one calculated assuming that poly(L-proline) displaced actin from profilin and in contrast was consistent with the formation of a ternary actin–profilin–poly(L-proline) complex. The fluorescence titration curves of profilin by poly(L-proline) obtained in the absence and in the presence of G-actin were superimposable (data not shown). In addition, the kinetics of interaction of G-actin with profilin in the presence of saturating amounts of poly(L-proline) yielded rate parameters identical to those determined in the absence of poly(L-proline) (Figure 4B,C). In conclusion, the affinity of G-actin for profilin is not affected by poly(L-proline) binding, which indicates, in agreement with the predictions from the structure (Schutt *et al.*, 1993), that these two ligands bind profilin in an energetically independent fashion.

Finally, the ability of profilin to promote F-actin assembly was assayed, as previously described (Pantaloni & Carlier, 1993), by measuring the steady-state amount of polymerized actin in the presence of 10 μM thymosin β_4 and profilin at different concentrations. Identical data shown in Figure 7 were obtained in the absence and presence of 0.2 mg/mL poly(L-proline) (i.e., a saturating amount), showing that the poly(L-proline)–profilin–actin complex participates in assembly at the barbed end in a manner identical to that of the profilin–actin complex.

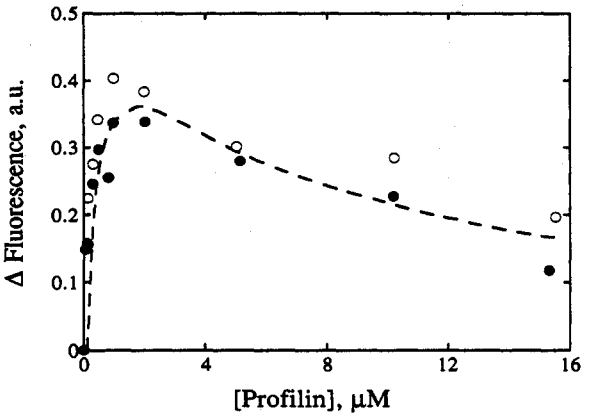

FIGURE 7: Poly(L-proline) does not affect the ability of profilin to promote F-actin assembly in the presence of thymosin β_4. The concentration of F-actin at steady state was measured after overnight incubation in samples containing 1.5 μM actin (1% pyrenyl labeled), 10 μM Tβ_4, and profilin at the indicated concentrations, in the presence (●) or absence (○) of 0.2 mg/mL poly(L-proline) (MW 10 000–30 000).

DISCUSSION

In this paper we show that intrinsic protein fluorescence has been used successfully to monitor actin–profilin interaction. This method is sensitive and well suited to measure protein–protein equilibrium dissociation constants in the submicromolar range, where other methods relying on protein assays are inaccurate. Although in many cases specific labeling of Cys374 (or Lys373) on G-actin with fluorescent probes (pyrene, AEDANS, NBD) has proven useful to monitor its interaction with a number of actin binding proteins, these probes cannot be used to monitor profilin binding due to the large decrease in affinity caused by modification of the C-terminus of actin (Malm, 1984). The change in protein fluorescence linked to complex formation also appears quite useful in monitoring the kinetics of the reaction. The identity of the tryptophans whose fluorescence is quenched in the complex is not known. Two tryptophans, W3 and W31 in human profilin sequence, are found in all profilins and are present in the highly conserved sequences that were initially, for that reason, thought to represent the actin binding site (Pollard & Rimm, 1991). However, the crystalline structure of the profilin–actin complex (Schutt *et al.*, 1993) leaves no doubt that these two tryptophans are not part of the actin–profilin interface; hence the fluorescence change recorded upon binding profilin to G-actin must be due to the shielding of some tryptophan(s) in actin exclusively, and not in profilin as we proposed in a preliminary report (Carlier *et al.*, 1993) before the structure of profilin–actin was known. The change in accessibility of actin tryptophans to solvent upon binding profilin strengthens this conclusion. A solvent-exposed tryptophan candidate on actin, W356, is located at the bottom of subdomain 1 in the region where profilin is in contact with profilin. The fluorescence quenching, which corresponds to a quenching of ~25% of the total fluorescence in the complex, directly monitors the bimolecular process of reaction of G-actin with profilin, rather than a subsequent conformation change, which supports the view that the quenched tryptophan(s) is (are) very close to the contact area. The linearity of the modified Stern–Volmer plot (Figure 3) suggests that a single tryptophan is quenched by KCl and hence by profilin binding.

Equilibrium and kinetic measurements indicate that the affinity of spleen profilin for muscle G-actin is very high, with a value of K_p of 0.1–0.25 μM, i.e., one order of magnitude lower than the reported values, which lie in the range 1–10 μM [see Machesky and Pollard (1993) for review]. The number we find here in low ionic strength buffer is nevertheless in good agreement with the values (0.3–0.6 μM) previously derived from kinetic and steady-state experiments performed under physiological ionic conditions (Pantaloni & Carlier, 1993; Pring *et al.*, 1992) under conditions where barbed ends were capped. The slight difference between the values of K_p found at 5 and 100 mM salt is consistent with the composite (ionic, polar, and hydrophobic) nature of the profilin–actin interface (Schutt *et al.*, 1993). We have earlier pointed out (Pantaloni & Carlier, 1993) that values of K_p derived from the shift in critical concentration plots under conditions where barbed ends were free were erroneous (too high by at least one order of magnitude) because the participation of profilin–actin complex in the maintenance of filament steady state was not considered. Hence independent methods converge toward the conclusion that the affinity of profilin for G-actin is of the order of 10^7 M^{-1}, much higher than previously thought, yet in good agreement with the large area (>2000 Å) of the interface and the large number (10) of hydrogen bonds between the two proteins in the crystalline profilin–actin complex. The profilin–actin complex studied here contains both nucleotide and divalent metal ion bound to actin. The measured affinities are practically identical for Ca- and Mg-actin in agreement with previous reports (Larsson & Lindberg, 1988) and also independently of whether ATP or ADP is bound to actin. On the other hand, in polymerization buffer, profilin was found to have a lower affinity for ADP-actin (Pantaloni & Carlier, 1993).

All data collected thus far show that, in the presence of at least micromolar amounts of free Ca-ATP, profilin–actin is saturated by CaATP and therefore is similar in structure to crystalline profilin–actin.

The bimolecular reaction of profilin with G-actin is diffusion-limited, with an association rate constant of 45 μM^{-1} s^{-1} at 20 °C. In agreement with the predictions from the structure (Schutt *et al.*, 1993; Cedergren-Zeppezauer *et al.*, 1994) and with mutagenesis studies (Haarer *et al.*, 1993; Björkegren *et al.*, 1993), binding of poly(L-proline) to profilin is totally independent of G-actin binding, i.e., neither the affinity nor the binding rate of G-actin for profilin are affected by poly(L-proline) binding. This independence of the binding sites appears both at low ionic strength and in the assembly test (Figure 7) which is performed under physiological ionic conditions. The large enhancement of both tryptophan and tyrosine fluorescences accompanying poly(L-proline) binding is consistent with W3, Y6, W31, and Y139 responding to poly(L-proline) binding independently of actin binding. Experiments with poly(L-proline) of different sizes show that a minimum of 10 covalently linked proline residues is necessary to obtain some binding with an intrinsic dissociation constant of 50 μM, in reasonable agreement with the value of 30 μM reported for *Acanthamoeba* profilin (Machesky & Pollard, 1993). A sequence of 10 prolines corresponds to three turns of the helix II structure of poly(L-proline). The above figures suggest that the tight binding of profilin to poly(L-proline)–agarose columns cannot be accounted for by a ligand size of only 10 prolines. Our data indicate that peptides of 15–20 prolines would bind with one order of magnitude higher affinity. This conclusion seems at variance with the very recent proposal (Metzler *et al.*, 1994), based on NMR data obtained at very high (10^{-3}M) concentrations of profilin and poly(L-proline), that a sequence of six prolines would be sufficient to bind to profilin. A sequence of 15 prolines in the helix II conformation would, however, span a distance of 47 Å, much

longer than the length of the solvent-exposed hydrophobic region on profilin. Hence the increased affinity of long polyprolines ($n > 10$) might be due to the presence of overlapping consecutive sites on these large peptides.

Proline-rich sequences which are known to bind SH_3 domains in proteins involved in signaling pathways generally consist of five consecutive prolines flanked by other amino acid residues specifying the binding to the relevant target. The ActA protein which is expressed at the surface of *Listeria* plays a crucial role in the propulsion of the bacterium (Kocks *et al.*, 1992) and was proposed to be involved in profilin binding (Thériot *et al.*, 1994). ActA contains a 4-fold repeated proline-rich peptide, in which $(Pro)_4$ sequences are flanked by asp and glu residues. Deletion of the four repeats is necessary to abolish movement of *Listeria* (Smith & Portnoy, 1993). We find that the proline-rich peptide 235–256 of ActA does not bind to the poly(L-proline) binding site of profilin up to 1 mM. Two possible reasons may account for this result: either profilin does not bind to the proline rich sequences of ActA and polyproline binding is not biologically relevant in profilin function, a conclusion also reached from mutation experiments (Haarer & Brown, 1993), or the 4-fold repeated polyproline motifs are spatially organized so as to allow the formation of a cluster of ~16 prolines at the surface of ActA, a number sufficient to ensure tight binding. Future experiments therefore are needed to clarify this point. However, it is interesting to note that polyproline binding does not modify the function of profilin as a motor of actin assembly, which involves association of the profilin–actin complex to the filament barbed ends. Hence theoretically profilin could shuttle actin subunits at the barbed end of actin filaments while being immobilized on a poly(L-proline) anchor.

ACKNOWLEDGMENT

We thank Drs. Pascale Cossart for a generous gift of ActA peptide 235–256, Dominique Pantaloni, Uno Lindberg, and Francis Rodier for helpful discussions, and Dr. Samoukov for synthesizing $(L\text{-Pro})_6$, $(L\text{-Pro})_8$, and $(L\text{-Pro})_{10}$.

REFERENCES

Björkegren, C., Rozycki, M., Schutt, C. E., Lindberg, U., & Karlsson, R. (1993) *FEBS Lett. 333*, 123–126.

Buss, F., Temm-Grove, C., Henning, S. & Jockusch, B. (1992) *Cell Motil. Cytoskeleton 22*, 51–61.

Cao, L., Babcock, G. C., Rubenstein, P. A., & Wang, Y. (1992) *J. Cell Biol. 117*, 1023–1029.

Carlier, M.-F., & Pantaloni, D. (1994) *Seminars in Cell Biology* (in press).

Carlier, M.-F., Pantaloni, D., & Korn, E. D. (1984) *J. Biol. Chem. 259*, 9983–9986.

Carlier, M.-F., Pantaloni, D., & Korn, E. D. (1986) *J. Biol. Chem. 261*, 10785–10792.

Carlier, M.-F., Blanchoin, L., Marchand, J.-B., & Pantaloni, D. (1993a) *Mol. Biol. Cell 4*, 149a.

Carlier, M.-F, Jean, C., Rieger, K.-J., Lenfant, M., & Pantaloni, D. (1993b) *Proc. Natl. Acad. Sci. U.S.A. 90*, 5034–5038.

Carlsson, L., Nystrom, L. E., Sundkvist, L., Markey, F., & Lindberg, U. (1977) *J. Mol. Biol. 115*, 465–483.

Cedergren-Zeppezauer, E. S., Goonesekere, N. C. W., Rozycki, M. D., Myslik, J. C., Dauter, Z., Lindberg, U., & Schutt, C. E. (1994) *J. Mol. Biol.* (in press).

Cooley, L., Verheyen, E., & Ayers, K. (1992) *Cell 69*, 173–184.

Finkel, T., Theriot, J. A., Dise, K. R., Tomaselli, G. F., & Goldschmidt-Clermont, P. J. (1994) *Proc. Natl. Acad. Sci. U.S.A. 91*, 1510–1514.

Goldschmidt-Clermont, P. J., Machesky, L. M., Baldassare, J. J., & Pollard, T. D. (1990) *Science 247*, 1575–1578.

Goldschmidt-Clermont, P. J., Machesky, L. M., Doberstein, S. K., & Pollard, T. D. (1991) *J. Cell Biol. 113*, 1081–1089.

Goldschmidt-Clermont, P. J., Furman, M. I., Wachsstock, D., Safer, D., Nachmias, V. T., & Pollard, T. D. (1992) *Mol. Biol. Cell 3*, 1015–1024.

Haarer, B. K., Lillie, S. H., Adams, A. E. M., Magdolen, V., Bandlow, W., & Brown, S. S. (1990) *J. Cell Biol. 110*, 105–114.

Haarer, B. K., Petzold, A. S., &Brown, S. S. (1993) *Mol. Cell. Biol. 13*, 7864–7873.

Haugwitz, M., Noegel, A. A., Karakesisoglou, J., &Schleicher, M. (1993) *Mol. Biol. Cell 4*, 3a.

Kaiser, D. A., Goldschmidt-Clermont, P. J., Levine, B. A., & Pollard, T. D. (1989) *Cell Motil. Cytoskeleton 14*, 251–262.

Kocks, C., Gouin, E., Tabouret, M., Berche, P., Ohayon, H., & Cossart, P. (1992) *Cell 68*, 521–531.

Kouyama, T., & Mihashi, K. (1981) *Eur. J. Biochem. 114*, 33–38.

Larsson, H., & Lindberg, U. (1988) *Biochim. Biophys. Acta 953*, 95–105.

Lassing, I., & Lindberg, U. (1985) *Nature 314*, 472–474.

Lehrer, S. S. (1971) *Biochemistry 10*, 3254–3263.

Lindberg, U., Schutt, C. E., Hellsten, E., Tjäder, A.-C., & Hult, T. (1988) *Biochim. Biophys. Acta 967*, 391–400.

Machesky, L. M., & Pollard, T. D. (1993) *Trends Cell Biol. 3*, 381–385.

Malm, B. (1984) *FEBS Lett. 173*, 399–402.

McLean-Fletcher, S., & Pollard, T. D. (1980) *Biochem. Biophys. Res. Commun. 96*, 18–27.

Metzler, W. J., Constantine, K. L., Friedrichs, M. S., Bell, A. J., Ernst, E., & Lavoie, T. B. (1993) *Biochemistry 32*, 13818–13829.

Metzler, W. J., Bell, A. J., Ernst, E., Lavoie, T. B., & Mueller, L. (1994) *J. Biol. Chem. 269*, 4620–4625.

Mockrin, S. C., & Korn, E. D. (1980) *Biochemistry 19*, 5359–5362.

Nishida, E. (1985) *Biochemistry 24*, 1160–1164.

Pantaloni, D., & Carlier, M.-F. (1993) *Cell 75*, 1007–1014.

Pollard, T. D., & Cooper, J. A. (1984) *Biochemistry 23*, 6631–6641.

Pollard, T. D., & Rimm, D. L. (1991) *Cell Motil. Cytoskeleton 20*, 169–177.

Pring, M., Weber, A., & Bubb, M. R. (1992) *Biochemistry 31*, 1827–1836.

Safer, D., Elzinga, M., & Nachmias, V. T. (1991) *J. Biol. Chem. 266*, 4029–4032.

Schutt, C. E., Myslik, J.-C., Rozycki, M. D., Goonesekere, N. C. W., & Lindberg, U. (1993) *Nature 365*, 810–816.

Smith, G. A., & Portnoy, D. A. (1993) *Mol. Biol. Cell 4*, 149a.

Spudich, J. A., & Watt, S. (1971) *J. Biol. Chem. 246*, 4866–4871.

Tanaka, M., & Shibata, H. (1985) *Eur. J. Biochem. 151*, 291–297.

Thériot, J. A., Rosenblatt, J., Portnoy, D. A., Goldschmidt-Clermont, P. J., & Mitchison, T. J. (1994) *Cell 76*, 505–517.

Valentin-Ranc, C., & Carlier, M.-F. (1989) *J. Biol. Chem. 264*, 20871–20880.

Vinson, V. K., Archer, S. J., Lattman, E. E., Pollard, T. D., & Torchia, D. A. (1993) *J. Cell Biol. 122*, 1277–1283.